



Mean Balance Ratio to Characterize Ground Motion Loading History for Performance Based Design

Arjun Jayaprakash¹, Mervyn J. Kowalsky²

¹ Ph.D. Candidate, Department of Civil, Construction and Environmental Engineering, NC State University, Raleigh, NC, United States.

² Professor, Department of Civil, Construction and Environmental Engineering, NC State University, Raleigh, NC, United States.

ABSTRACT

Accurate characterization of seismic hazards and structural performance limit states are imperative to achieve best results in performance based seismic design. Seismic hazards have been characterized in the past utilizing seismic intensity measures such as peak ground accelerations, spectral accelerations, spectral displacements etc. Recent studies have revealed the impact of ground motion loading history on performance limit states such as longitudinal reinforcement bar-buckling in RC bridge columns. Conventional hazard characterizations provide only peak values and therefore fall short in providing necessary ground motion information to account for these effects. This study tries to move towards alternate parameters that could potentially be utilized to reproduce loading history characteristics of ground motions from conventional peak parameters, when necessary. A parameter named Mean Balance Ratio was investigated for potential utility. 1554 ground motion records were obtained from the PEER NGAwest2 ground motion database. The records spanned moment magnitudes 4.0 to 7.9 and epicentral distances 0.1 km to 400 km. The impact of magnitude, epicentral distance, initial elastic time-period, system type, and system ductility on mean balance ratio was investigated and some useful trends were identified. It was found that the structural period, limit state ductility and epicentral distance are important variables that explain the variation in mean balance ratio. Implications of characterizing mean balance ratio from performance based design standpoint is also discussed.

Keywords: Seismic hazard characterization, Mean Balance Ratio, Loading history effects, Performance based design, Statistical inference

INTRODUCTION

Seismic hazard has been characterized for design in several ways. Intensity measures (IM) that provide single numerical values such as peak ground acceleration (PGA), peak spectral acceleration (S_a), significant duration, Arias intensity etc. have been useful in estimating the level of hazard for a given structure. These parameters are utilized in either a deterministic or a probabilistic framework to obtain a design level hazard. However, one IM by itself does not provide enough information to fully characterize a hazard. Each measure preserves specific aspects of seismic hazard while losing others.

Seismic hazard is also characterized through time-histories of ground acceleration or displacement that preserve all characteristics of real ground motions. These time-histories are recorded by recording stations during earthquake events. This method of characterization, albeit having all information preserved, is of minimal use by themselves in the design process. This is because the recurring likelihood of past ground motions is close to non-existent.

Most common IMs in current use are PGA, S_a and S_d of which the latter two have gained popularity from the perspective of performance based seismic design (PBSD). PBSD consists of a set of engineering procedures for design, construction and maintenance of structures to achieve predictable levels of performance in response to specific levels of earthquake within definable levels of reliability [1]. A design philosophy that can be incorporated seamlessly into PBSD is the direct displacement based design (DDBD). DDBD combines hazard characterizations with structural performance limit state models to achieve desired levels of structural performance under seismic events. Two requirements of DDBD are:

1. Well defined structural performance limit states, and
2. Accurate hazard characterizations.

Research on both these requirements are conventionally performed separately. However, developments in one are complemented by studies in the other. Recent studies have revealed the impact of seismic loading history on the damage control performance limit state in reinforced concrete (RC) bridge columns [2-4].

In the case of reinforced concrete (RC) bridge columns, a key performance limit state is the onset of reinforcement bar buckling. Studies by Feng et al. [3] and Goodnight et al. [4] revealed the importance of seismic loading history in buckling limit state determination. Earlier, Moyer and Kowalsky [5] had observed the influence of tensile strains on the onset of bar buckling, and described a tension-based buckling mechanism where a reinforcement bar exceeds a certain tensile strain limit before the onset of buckling occurs upon load reversal. These studies [3, 4 and 6] have also revealed an additional mechanism where a high compressive strain demand on extreme bars force the accompanying transverse steel to yield, thereby changing the boundary conditions of the longitudinal steel. This causes premature buckling during a subsequent compression cycle if a certain tensile strain (lower than previously predicted in [5] is attained on any preceding tension cycle. Feng et al. [3] provided an empirical model that takes this mechanism into account. This model provides equations for tensile strain limits corresponding to preceding peak compressive strains. Using the plastic hinge method [7], these peak compressive and tensile strain pairs of extreme bars can be related to the peak displacements of columns on either side of the starting position. IMs such as S_a and S_d only provide peak response values and therefore limit the utility of such a model. Currently, this model is being used for design assuming equal displacement on both sides.

To be in line with performance-based design principles, i.e., being able to accurately predict the performance of a structure under a given hazard, more refinements in limit state characterization are imminent. Since earthquakes are cyclic in nature, these refined limit state definitions will inevitably account for the uncertainties caused due to cyclic response such as imbalance. This study aims to move towards characterizing hazards to provide valuable input parameters for the Feng et al. [3] model as well as other future limit state models that account for the impact of ground motion loading history. There have been a few studies that investigated seismic hazard characterizations that account for the cyclic nature of ground motions. These include effective number of cycles [8,9], effective cyclic energy [10], damage based inelastic spectra [11] etc. Insofar as the authors are aware, these characterizations were developed from the perspective of force-based or energy-based seismic design philosophies. Spectral accelerations and ground motion durations were given major focus and many were developed with the goal of controlling site characteristics such as soil liquefaction. The mean balance ratio approach discussed herein has evolved within the displacement-based framework to address a very specific problem of response imbalance. It is important to recognize the difference between each approach and use them when required.

RESEARCH APPROACH

Dataset

A large suite of earthquake ground motions (1554 GMs) were obtained from PEER NGA-West2 database [12] for this study. The ground motions were chosen so that the dataset would consist of records that have a wide range of magnitudes (M_w) and closest distance parameters (D). Figure 1(a) shows a scatter plot of M_w and D pairs of all the records in this dataset. After preliminary analysis, a smaller subset of the full dataset was subsequently chosen to perform non-linear time history (NLTH) analysis which is discussed later. Figure 1(b) shows a similar plot for the partial dataset.

Balance Ratio (R_b)

To capture some of the loading history characteristics of ground motions, a parameter was defined called the *Balance Ratio* (R_b). R_b is defined as the ratio of the absolute values of the peak displacements on either side of the initial position of a single-degree-of-freedom (SDOF) oscillator under a ground motion input. It is convenient to place the larger number on the numerator to always obtain R_b values greater than 1.0. Figure 2 shows a sample displacement time-history of a non-linear SDOF oscillator. The positive and negative peaks are marked with red circles. For this specific response, the R_b , which in this case is the ratio of the positive peak to the negative peak, will be close to 3.5.

Balance Ratio (R_b) provides a simple quantification of the imbalance in structural response to ground motions. Current practice in DDBD is to design structures by either neglecting the effect of imbalance or by assuming that the responses are balanced ($R_b = 1.0$). Figure 2 suggests the possibility of imbalance or higher R_b values. Studying a large dataset of ground motions provided further insight into the imbalance in structural response to ground motions.

Dynamic Analysis

First, all 1554 ground motions were analyzed to obtain the elastic R_b for all records for a period range of 0.1s to 10s. This was done by modifying a MATLAB code that generated response spectra to also calculate the ratio of peak displacements in both directions. Effectively, this was equivalent to performing linear time history (LTH) analysis on SDOF oscillators within the period range utilizing each of the 1554 ground motions uni-directionally. There was a total of 100 elastic SDOF systems between the period range of 0.1s to 10.0s. Later, non-linear time history (NLTH) analysis was performed on SDOF systems

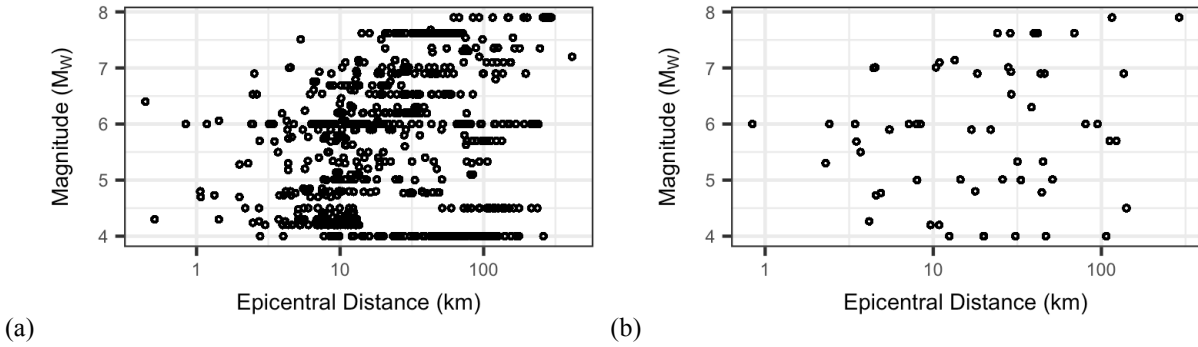


Figure 1. Magnitude versus Distance for the two GM datasets used in this study (a) Full Dataset, (b) Data subset used for NLTH Analyses.

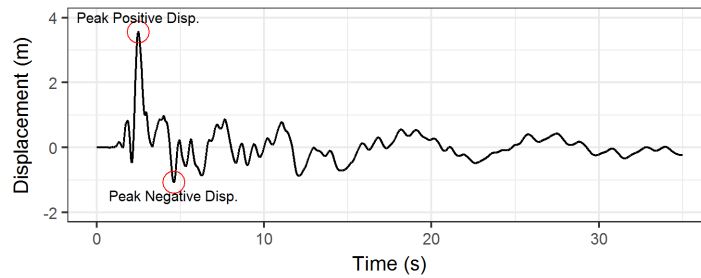


Figure 2. A sample displacement time history of a non-linear SDOF oscillator with positive and negative peaks annotated.

with five different section hysteresis rules utilizing a smaller subset of 120 ground motions that were sampled from the available 1554 ground motions. Five different hysteresis rules that were utilized included Bilinear, Ramberg-Osgood, Thin-Takeda, Large-Takeda and Flag-shaped hysteretic models. These SDOF systems were within a period range of 0.25s to 10.0s. There was a total of 20 different time period values. The results were studied collectively using a probabilistic approach of random sampling to reveal trends in the data.

Statistical Analysis

Two separate datasets were created as a result of linear and non-linear time-history analysis of SDOF systems. These two datasets formed the population for random sampling and analysis. 2000 random samples from both populations were selected with a sample size n equal to 2000. These samples were collated together to form two large datasets, linear and non-linear, of 4 million observations of R_b . The effect of magnitude (M_w), epicentral distance (D), initial elastic time period (T), maximum displacement ductility (μ_{Δ}) and the system type (non-linear hysteresis rule) on *Mean Balance Ratio* (μ_{R_b}) was investigated. Results from such approach are predicated on the assumption that the assembled population is a reasonable representation of real active shallow crustal events. These results are discussed in the following section.

RESULTS

Mean Balance Ratio (μ_{R_b})

Mean Balance Ratio (μ_{R_b}) is defined as the mean value of any probability distribution of R_b . The central limit theorem in statistics states that the sample mean for any parameter tends to be normally distributed given a large enough sample size. Thus, μ_{R_b} is a convenient parameter to investigate from a predictive perspective. Inference on μ_{R_b} was performed through an estimator ($\hat{\mu}_{R_b}$) which was defined as the arithmetic mean of all R_b values within a random sample obtained from the base population. Figure 3 shows the distribution of $\hat{\mu}_{R_b}$ in the sampled data. Figure 3(a) shows the empirical distribution of $\hat{\mu}_{R_b}$ obtained from linear time history (LTH) analyses while Figure 3(b) shows the empirical distribution of $\hat{\mu}_{R_b}$ obtained from non-linear time history (NLTH) analyses. For linear systems, the average value of $\hat{\mu}_{R_b}$ was 1.26 and for non-linear systems it was 1.46. These values clearly deviate from the current assumption of $\hat{\mu}_{R_b}$ equal to 1.0.

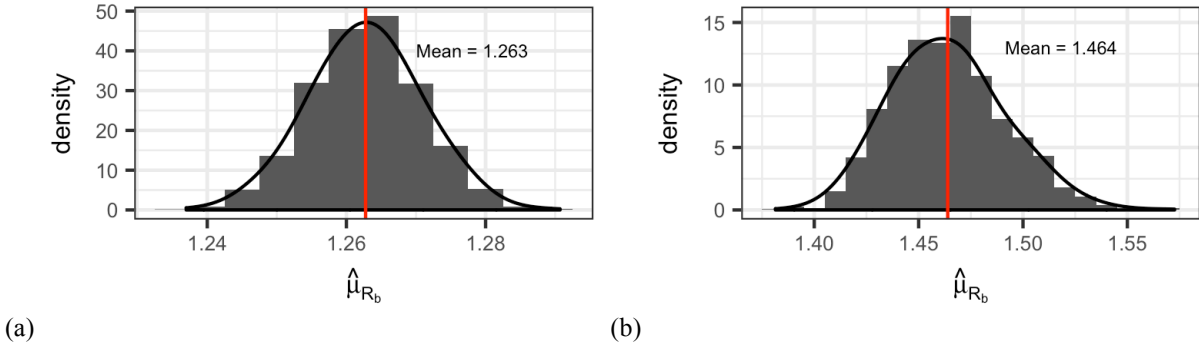


Figure 3. Probability density of $\hat{\mu}_{Rb}$ obtained from empirical data obtained from (a) LTH analyses and (b) NLTH analyses.

Table 1. Average values of Mean Balance Ratio for different variables independently.

| Magnitude Bins | Mean Value | Epicentral Distance Bins | Mean Value | Hysteresis Rule | Mean Value | Ductility Range | Mean Value |
|----------------|------------|--------------------------|------------|-----------------|------------|-----------------|------------|
| Magnitude 4 | 1.37 | 0 to 5 km | 1.40 | Bilinear | 1.56 | μ_1 | 1.58 |
| Magnitude 5 | 1.32 | 5 to 10 km | 1.42 | Flag-Shaped | 1.37 | μ_2 | 1.83 |
| Magnitude 6 | 1.21 | 10 to 15 km | 1.33 | Ramberg-Osgood | 1.42 | μ_3 | 2.12 |
| Magnitude 7 | 1.14 | 15 to 25 km | 1.25 | Large Takeda | 1.52 | μ_4 | 2.80 |
| | | 25 to 40 km | 1.20 | Thin Takeda | 1.48 | μ_5 | 2.59 |
| | | 40 to 60 km | 1.16 | | | | |
| | | 60 to 90 km | 1.19 | | | | |
| | | Greater than 90 km | 1.16 | | | | |

The mean balance ratio provides an estimate for the average imbalance of structural response over a large number of ground motions. Real values of R_b could potentially be much larger. This motivated further investigation into the data to assess the impact of different variables on response imbalance.

Influence of Event Magnitude (M_w)

To isolate the effects of seismic source characteristics, the data obtained from LTH analysis was utilized. This eliminated any influence of non-linear characteristics of structural response. The event magnitude was categorized into four different bins as shown in the first part of Table 1. Table 1 shows the average values of $\hat{\mu}_{Rb}$ within bins of different variables independently. These variables are discussed in detail subsequently. The M_w corresponding to each ground motion was rounded down to the nearest lower integer. For e.g., an M_w of 5.8 was categorized into the Magnitude 5 bin. $\hat{\mu}_{Rb}$ was calculated by finding the arithmetic mean of the observations corresponding to each magnitude bin in each of the 2000 random samples. Figure 4 shows the empirical probability density of $\hat{\mu}_{Rb}$ for each magnitude bin. The location of the peak of the distribution, which is equal to the mean value of the statistic under the normality assumption, decreases with increasing event magnitude. In addition, the distribution also gets narrower with increasing event magnitude. This suggests that potentially a more balanced structural response could be expected for larger event magnitudes. The response in terms of imbalance may also be more predictable at higher event magnitudes.

Further inquiry is necessary to make any conclusions on the effect of magnitude. A large proportion of high magnitude events in the database are caused by reverse faulting mechanism while for lower magnitude events, the dominant cause is strike-slip faulting mechanism. Fault type was not given special attention to when the data was sampled. Lack of control on the proportion of fault type in each sample may have lead to some bias in the results. Similarly, at large epicentral distances, $\hat{\mu}_{Rb}$ reduces and approaches 1.0. This is discussed later. The sample for high magnitude events could have been influenced by the presence of a larger proportion of far-field recordings. Low magnitude earthquakes have minimal effect at long distances and hence the random samples may have a larger proportion of near-field earthquakes. Further studies are ongoing to address these issues.

Influence of Site Epicentral Distance (D)

Epicentral distances of the records were classified into eight different categorical bins as shown in the second part of Table 1. Finer bins close to the epicenter and coarser ones farther away allowed a consistent proportion of observations in each bin. $\hat{\mu}_{Rb}$ was calculated by finding the arithmetic mean of the observations corresponding to each distance bin in each of the 2000

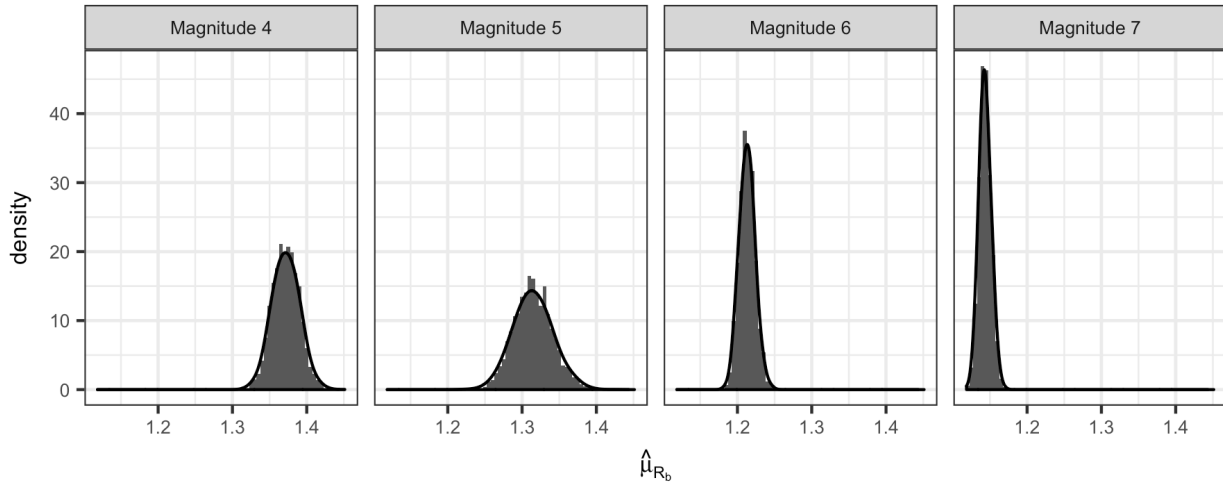


Figure 4. Probability density of $\hat{\mu}_{Rb}$ for each magnitude bin defined in this study.

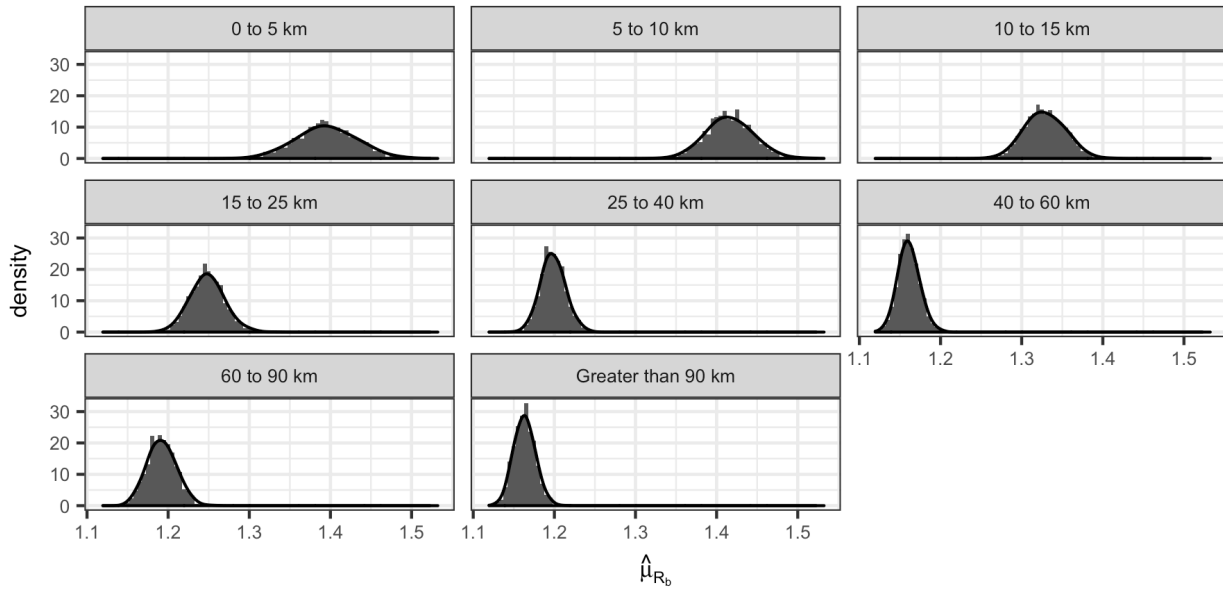


Figure 5. Probability density of $\hat{\mu}_{Rb}$ for each distance bin defined in this study.

random samples. Figure 5 shows the empirical probability density of $\hat{\mu}_{Rb}$ for each of the different distance bins. $\hat{\mu}_{Rb}$ is higher for near-fault events and has a wider distribution. As the records are farther away from the epicenter, $\hat{\mu}_{Rb}$ decreases. This is in line with expectation since near-fault records may also be influenced by forward directivity effects such as *velocity pulses* or *flings*. This would force the response to be unbalanced. This can be tested by using appropriate datasets controlling for forward directivity effects. This is currently being studied.

Influence of System Type (Hysteresis Rules)

Five different non-linear structural systems (hysteretic rules) were utilized to perform NLTH analysis on SDOF systems. The hysteretic rules that were chosen are provided in the third part of Table 1. Figure 6 shows the empirical probability density of $\hat{\mu}_{Rb}$ for all five structural systems. The mean values of $\hat{\mu}_{Rb}$ for all systems range between 1.37 to 1.56 (Table 1) which deviate from a balanced response of 1.0. The lower tails of all five distributions fall above 1.30 which suggest that the likelihood for a balanced response, i.e., having peaks of equal displacement in both sides, for any of these five structural systems is extremely

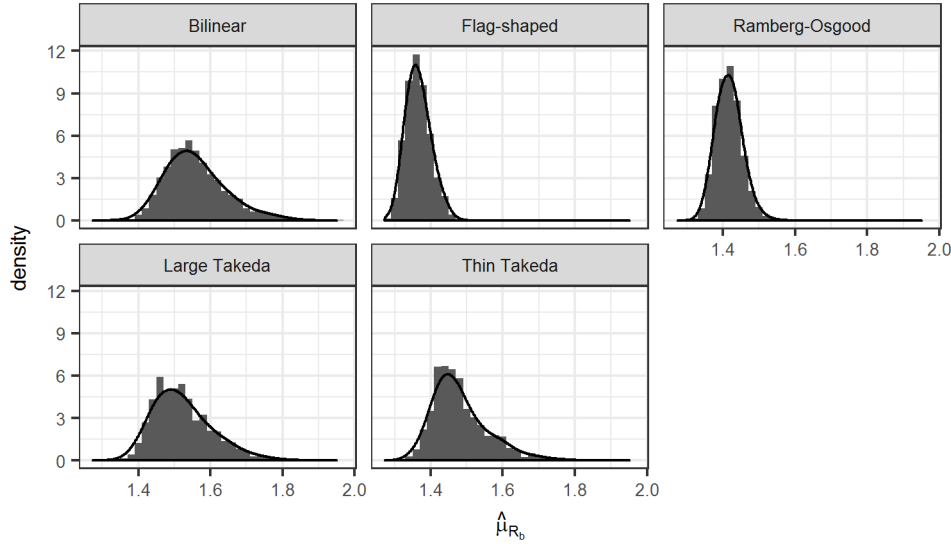


Figure 6. Probability density of $\hat{\mu}_{Rb}$ for different section hysteretic rules used in NLTH analysis.

low. Both Flag-shaped and Ramberg-Osgood systems show narrow distributions while the other three systems have a wider base.

Influence of System Displacement Ductility (μ_{Δ})

The variability in system ductility was achieved indirectly in NLTH analysis. The dynamic analysis program *Ruaumoko* [13] was used to perform NLTH analysis. SDOF systems were defined with two different yield strengths: 1000 kN-m and 2000 kN-m. Two each of reinforced concrete and structural steel (for Ramberg-Osgood) sections that possessed these strengths were selected through trial and error moment-curvature analysis. The moment-curvature analysis also provided the first yield and in turn the equivalent yield curvatures for each section. The equivalent yield displacement of an SDOF column in single bending is given by Eq. (1) where Δ_y is the equivalent yield displacement, ϕ_y is the yield curvature and L is the length of the column. SDOF columns of various lengths were chosen to obtain the different time period values ranging from 0.25s to 10.0s. For each different SDOF system, the system ductility (μ_{Δ}) was calculated by dividing the peak displacement obtained from NLTH analysis by its equivalent yield displacement (Δ_y). The result was a continuous random variable starting from values close to zero that went up to extremely high values of around 20. These high ductilities are meaningless in a physical sense. In reality, the maximum ductility values for ductile systems are normally be less than 8 and typically between 3 and 5.

$$\Delta_y = \frac{\phi_y L^2}{3} \quad (1)$$

For convenience in understanding the influence of ductility on $\hat{\mu}_{Rb}$, the continuous variable of system ductility was converted into categorical bins as shown in the fourth part of Table 1. A ductility value that lay between 2.5 and 3.5, for instance, was classified into ductility 3 ($\mu_{\Delta 3}$) bin. Please note that the ductility variable indicates the maximum ductility achieved by the SDOF system.

Figure 7 shows the probability distribution of $\hat{\mu}_{Rb}$ for systems in each ductility level. $\mu_{\Delta 1}$ systems that are either close to yielding or have just yielded show the lowest values of $\hat{\mu}_{Rb}$ with a narrow distribution while higher ductilities such as $\mu_{\Delta 4}$ and $\mu_{\Delta 5}$ show very high values of $\hat{\mu}_{Rb}$ with wider distributions. Depending on the maximum ductility of interest, the expectation for balance or imbalance of structural response changes. For e.g., from the perspective of damage control limit state of reinforcement bar-buckling in RC bridge columns, the ductility level at which the limit state is designed to occur typically ranges between $\mu_{\Delta 3}$ to $\mu_{\Delta 5}$. Hence, at this level, a large imbalance between peaks on both directions should be accounted for in the DDBD process.

Influence of Initial Elastic Time Period (T)

For LTH analysis utilizing the large GM dataset, SDOF systems with 100 different T values were analyzed. These ranged between 0.1s and 10.0s at an increment of 0.1s. For NLTH analysis utilizing the GM data subset, SDOF systems with 20 different T values were analyzed. These were the initial elastic time periods for each non-linear system. The T values ranged between 0.25s to 10.0s. A larger proportion of these were within the short period range. After random sampling, the empirical

probability density of $\hat{\mu}_{RB}$ for each T was calculated. The mean values and their two-sided 95% confidence limits (CL) are shown in Figure 8 for both linear and non-linear systems. As the structural period gets longer, there is a higher likelihood of observing imbalance in the peak displacements on both sides. Also, for the same initial elastic time period, a non-linear SDOF system has a larger $\hat{\mu}_{RB}$ compared to a linear system. From a design standpoint, if the initial elastic time period of the equivalent SDOF structure is known, this result implies that one can be 95% confident that the parameter μ_{RB} falls within the region bounded by the confidence limits given in Figure 8.

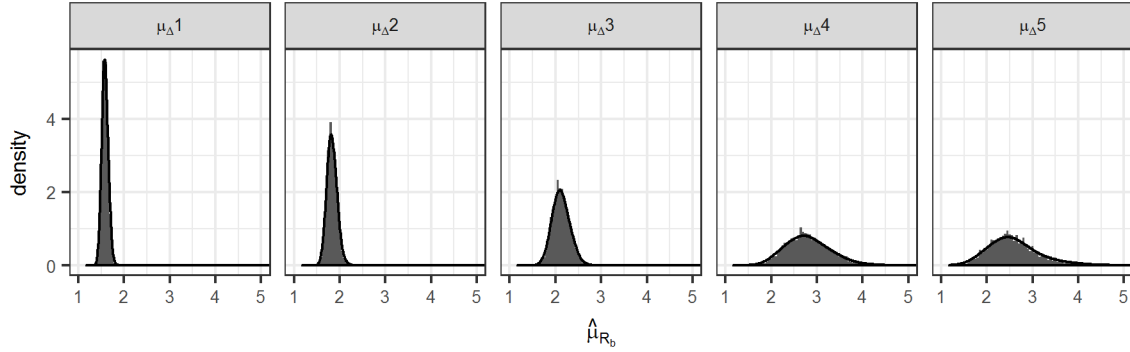


Figure 7. Probability density of $\hat{\mu}_{RB}$ at different displacement ductility levels of non-linear systems.

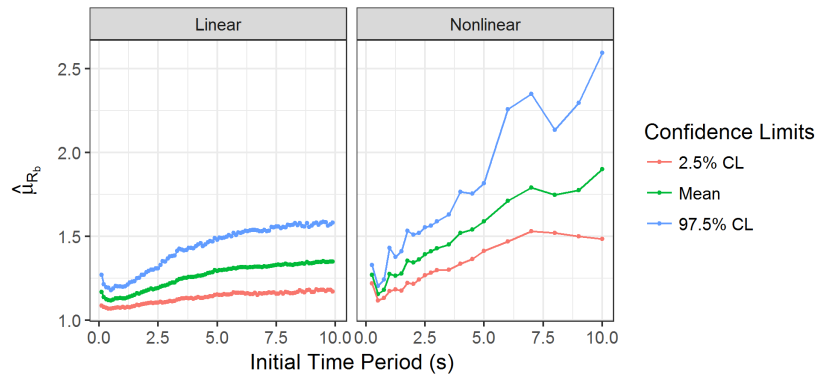


Figure 8. $\hat{\mu}_{RB}$ versus initial elastic time period (t) of the sdoF system from nlth analyses. Mean value of $\hat{\mu}_{RB}$ is shown alongside the 2.5% and 97.5% confidence limits.

Both linear and non-linear curves in Figure 8 show a dip in $\hat{\mu}_{RB}$ values at very short periods. In other words, the curves are not continuously increasing. This behavior requires further investigation within the very short period range. This could be a consequence of extremely small values of relative displacement for very rigid structures. R_b is a ratio of the peak displacements on both sides. The sensitivity of this parameter is higher for extremely small values of the numerator and denominator, which is the case with the peak relative displacement values for rigid structures. This could be a plausible explanation for observing slightly higher $\hat{\mu}_{RB}$ for very short periods compared to short periods.

IMPLICATIONS, CONCLUSIONS AND FUTURE WORK

Implications for Direct Displacement-based Design

Ground motions are erratic. Structural response under ground motions do not have equal displacements on either side of the equilibrium point. *Balance Ratio* (R_b) of a ground motion provides information regarding the opposite peak parameters when provided with conventional peak parameters. From the perspective of DDBD, structural displacement is an important quantity. Therefore, this study exclusively investigates R_b for displacements. For prediction models, a more useful parameter is the *Mean*

Balance Ratio (μ_{Rb}) that provides the same information as R_b , but as a statistical average. The implications of characterizing ground motion response in such a way can be better understood through an example.

The process of DDBD relies on structural limit state characterizations that can be related to structural displacements. For instance, this paper specifically refers to the damage control limit state of longitudinal reinforcement bar buckling in circular RC bridge columns. Using the Feng et al. [3] model, one can form equations for displacement limits on one side given the peak displacement achieved on the other side of equilibrium. This implies that to efficiently utilize this model in the design process, an engineer will require a hazard definition that provides information regarding peak displacements on both sides of equilibrium. If one were to characterize the parameter μ_{Rb} as a function of other known variables such as initial elastic time period (T), the target displacement ductility (μ_A), source-to-site closest distance parameter (D), event magnitude (M_w) etc., not unlike conventional ground motion prediction equations (GMPE), the efficiency of limit state models such as the Feng et al. [3] model can be increased.

Conclusions

A parameter termed as the *Mean Balance Ratio* (μ_{Rb}) was introduced in this paper. μ_{Rb} provides seismic designers with additional information regarding ground motion hazard, i.e., a scalar by which the peak displacement (or any response quantity) on one side of the equilibrium position of a SDOF oscillator can be multiplied with to obtain the peak on the opposite side. The motivation behind the need for such a parameter in DDBD was discussed. This was followed by analysis of a large dataset of ground motions obtained from the NGA-west2 database for active shallow crustal earthquakes utilizing a probabilistic approach. The probability distribution of μ_{Rb} was investigated independently for different variables that could potentially affect μ_{Rb} . Results revealed trends in the behavior of μ_{Rb} which have been displayed in a graphical form. It was shown that the current assumption of equal peaks on both sides of equilibrium is false. Implications of the study on DDBD were also discussed.

Future Work

The final goal of the study is to generate expressions for μ_{Rb} that would provide likelihoods of observing certain levels of imbalance in structural response. A rigorous statistical approach will be required to accomplish this which would involve regression models and model selection techniques. Work is underway to determine the relationship between the predictor variables and if there are other variables that contribute to the variation in μ_{Rb} . Simultaneously, the utility of μ_{Rb} in the design process is also being investigated.

REFERENCES

- [1] SEAOC Vision 2000 Committee et al. (1995). "Performance Based Seismic Engineering". *Structural Engineers Association of California, Sacramento, California*.
- [2] Syntzirma, D.V., Pantazopoulou, S.J., and Aschheim, M., (2009). "Load-history effects on deformation capacity of flexural members limited by bar-buckling". *Journal of Structural Engineering*, 136(1):1-11.
- [3] Feng, Y., Kowalsky, M.J., and Nau, J.M. (2014) "Effect of seismic load history on deformation limit states for longitudinal bar-buckling in rc circular columns". *Journal of Structural Engineering*, 141(8):04014187.
- [4] Goodnight, J.C., Kowalsky, M.J., and Nau, J.M. (2013). "Effect of load history on performance limit states of circular bridge columns". *Journal of Bridge Engineering*. 18(12):1383-1396.
- [5] Moyer, M.J., and Kowalsky, M.J. (2003). "Influence of tension strain on buckling of reinforcement in concrete columns". *ACI Structural Journal*. 100(1):75-85.
- [6] Feng, Y., Kowalsky, M.J., and Nau, J.M. (2014). "Finite-element method to predict reinforcing bar buckling in rc structures". *Journal of Structural Engineering*, 141(5):04014147, 2014.
- [7] Priestley, M.J.N., Calvi, G.M., and Kowalsky, M.J. (2007). "Direct displacement-based seismic design of structures". *IUSS Press, Pavia*
- [8] Hancock, J., and Bommer, J.J., (2005) "The effective number of cycles of earthquake ground motion". *Earthquake Engineering and Structural Dynamics*, 34(6):637-664.
- [9] Du, W., and Wang, G., (2017). "Empirical correlations between the effective number of cycles and other intensity measures of ground motions". *Soil Dynamics and Earthquake Engineering*, 102:65-74.
- [10] Kalkan, E., and Kunnath, S.K., (2007). "Effective cyclic energy as a measure of seismic demand". *Journal of Earthquake Engineering*, 11(5):725-751.
- [11] Greco, R., and Marano, G.C., (2015) "Inelastic seismic spectra including damage criterion: A stochastic approach". *Soil Dynamics and Earthquake Engineering*, 70:75-79.
- [12] Ancheta, T.D., Darragh, R.B., Stewart, J.P., Seyhan, E., Silva, W.J., Chiou, B.S.-J., Wooddell, K.E., Graves, R.W., Kottke, A.R., Boore, D.M., et al. (2014) "NGA-west2 database". *Earthquake Spectra*. 30(3):989-1005.
- [13] Carr, A.J. (2008) "Ruaumoko-inelastic dynamic analysis program". *Department of Civil Engineering, University of Canterbury, Christchurch, New Zealand*.